International Information and Engineering Technology Association
Advancing the World of Information and Engineering

Ingénierie des Systèmes d'Information
Vol. 30, No. 9, September, 2025, pp. 2223-2232
Journal homepage: http://iieta.org/journals/isi

Low-Power Hybrid CORDIC-DCT and CAVLC-Based Image Compression for Real-Time Wireless Capsule Endoscopy

Harshitha Shivaprasad[1], U. B. Mahadevaswamy[2*], Mallikarjunaswamy Srikantaswamy[3]

[1] Department of Electronics and Instrumentation Engineering, JSS Academy of Technical Education, Bengaluru 560060, India
[2] Department Electronics and Communication Engineering, JSS Science and Technology University, Mysuru 570006, India
[3] Department of Electronics and Communication Engineering, JSS Academy of Technical Education, Bengaluru 560060, India

Corresponding Author Email: mahadevaswamy@sjce.ac.in

https://doi.org/10.18280/isi.300902

Received: 25 June 2025
Revised: 21 August 2025
Accepted: 10 September 2025
Available online: 30 September 2025

Keywords:
wireless capsule endoscopy (WCE), discrete wavelet transform (DWT), coordinate rotation digital computer (CORDIC), Loeffler discrete cosine transform (DCT), context-adaptive variable length coding (CAVLC), energy-efficient compression, PSNR, medical image transmission

ABSTRACT

Wireless capsule endoscopy (WCE) is significantly challenged in transmitting massive amounts of gastrointestinal image information because of low bandwidth and power limitations in the capsule battery. Effective compression becomes mandatory in reducing storage needs, shortening transmission durations, and prolonging device use life with retained diagnostic image quality. This work describes a low-power hybrid image compression approach designed for real-time WCE applications. The novel approach combines a 5/3 lifting-based discrete wavelet transform (DWT) for multi-resolution image analysis, a coordinate rotation digital computer (CORDIC)-based Loeffler discrete cosine transform (DCT) for energy-efficient frequency-domain transformation, and context-adaptive variable length coding (CAVLC) for adaptive entropy coding. The approach harnesses the power of DWT space-frequency localization, DCT energy compaction, and CAVLC context-based redundancy reduction to obtain high compression ratios with negligible loss of fidelity. Experimental tests on standard endoscopic dataset benchmarks reveal the performance superiority of the approach over standard JPEG, JPEG2000, and DWT or DCT standalone methods, obtaining up to a 10× compression ratio with a peak signal-to-noise ratio (PSNR) of 36 dB, and with power consumption of only 0.75 W per image. These findings reveal the approach suitability for energy-efficient, hardware-friendly, and real-time WCE applications.

1. INTRODUCTION

Wireless capsule endoscopy (WCE) is the latest non-invasive diagnostic instrument employed to obtain detailed images of the GI tract. The capsule, with inbuilt miniature camera, source of light, transmitter, and battery, is ingested by the patient and sends images wirelessly as it makes its way along the GI tract. WCE greatly helps in diagnosing internal diseases like bleeding, tumors, ulcers, and Crohn's disease. Yet, one of the primary challenges of WCE is in the effective transmission and storage of the huge amounts of images created during operation, commonly more than 50,000 frames in each session. Because of the capsule's battery limitations and low available bandwidth, compression of images is the key factor in providing extended operation and efficient data handling [1]. Conventional techniques such as JPEG and JPEG2000 provide generic compression but are afflicted with problems such as blocking artifacts and excessive power use and are not well adapted to real-time embedded systems such as WCE [2]. To overcome such limitations, this paper introduces a new hybrid image compression method that combines three main components: the DWT based on the 5/3 Lifting Scheme, CORDIC-based Loeffler DCT, and CAVLC. The DWT is capable of capturing both spatial and frequency content by performing multi-resolution analysis, CORDIC-Loeffler DCT is able to perform efficient transformation with low computational complexity, and CAVLC is able to perform adaptive entropy encoding with high efficiency [3]. This hybrid technique is intended to increase the compression ratio with minimal loss of important diagnostic information, as tested under measures like peak signal-to-noise ratio (PSNR) and power consumption. The method proposed performs better in comparison with standalone compression methods and is well suited to power-constrained medical imaging contexts like WCE [4].

1.1 Research gaps

Our hybrid strategy optimally fills the research gaps by merging the respective strengths of 5/3 lifting-based DWT, CORDIC-Loeffler DCT, and CAVLC entropy coding in a single framework [5]. The multi-resolution analysis of DWT optimally preserves the diagnostically relevant low-frequency information and discards the redundant high-frequency information, thus reducing the noise sensitivity and poor energy compaction of standalone wavelet schemes. Low-complexity, hardware-friendly frequency transformation is realized by the CORDIC-Loeffler DCT, removing the blocking artifacts and numerical complexity of standard DCT implementations and enhancing energy efficiency for low-power WCE devices [6]. Lastly, adaptive entropy coding by CAVLC optimally takes advantage of the statistical characteristics of medical images dynamically without sacrificing image quality, and hence achieves superior compression without image quality degradation. The resultant balanced optimization of compression ratio, image quality, and power is then optimally suited for real-time, low-power WCE applications where established methods fall short of expectations.

1.2 Related work

Long et al. [7] suggested guide image and fraction-power transformation-based adaptive image enhancement in the case of wireless capsule endoscopy (WCE). Their adaptive guide image enhancement (AGIE) method improves low-contrast endoscopic images effectively by looking to high-quality exemplar images. The algorithm showed improvement of 64.20% in average intensity and performed better than all existing methods. Yet, the use of guide images of related scenes may be inhibiting in the case of real-time use with missing exemplar images. Diamantis et al. [8] proposed a new variational autoencoder (VAE) model, dubbed TIDE, to produce realistic WCE images. In contrast to traditional data augmentation based on GAN, the proposed model is able to produce realistic artificial images that are substitutable for training classifiers. The method facilitates dataset diversification and clinical verification. However, the process remains reliant on sophisticated architectures and computational power, which can be restrictive in low-power settings. Wu et al. [9] proposed an automatic hookworm detection method on WCE images based on multi-scale dual matched filters and Rusboost classification. The novelty of the work is that intensity histograms and region detection are combined to detect hookworms with high sensitivity. Although efficient, the performance of the model is liable to drop with extreme GI tract variations and untrained parasite morphs in the case of dataset dependency. Oliveira et. al. [10] experimented with estimating WCE capsule's 3D motion by frame registration on experimental porcine data. Their uniqueness is in estimating motion trajectories from mere sequences of images without any external tracking systems. But the level of accuracy would depend highly on the absence of noise, clearness of images, and immediacy of relative changes, and thus it cannot be highly robust in various real-time settings. Sushma and Aparna [11] suggested a video summarization method based on deep learning with convolutional autoencoders and motion analysis. The novelty is in the use of unsupervised deep feature extraction and structured keyframe selection with superior F-measure and compression rate. A weakness is that summarization is based on thresholds that are not supervised and therefore might not generalize well to different datasets or clinical settings. Varam et al. [12] employed Explainable AI (XAI) techniques to classify images of WCE employing transfer learning and visual explainability tools such as GradCAM and SHAP. Their technique increases confidence in prediction by making decisions transparent, with as high as 97% F1-score. The disadvantage is the reliance on pre-trained models and computationally intensive visualization modules, which is not practical in on-device diagnostics of resource-limited WCE devices. Orlando et al. [13] proposed a low-power, real-time architecture of the Hough Transform-based detection of polyps in HD WCE images. When implemented on an FPGA, the design provides shape-based ROI detection with low-energy consumption. Although with great integration potential, detection of interest is restricted to circular features and, therefore, can overlook irregular or planar lesions found in GI tract imaging. Peng et al. [14] proposed dual-band impulse radio-based coil antennas for MHz-band communication in WCE to improve data transmission with minimal loss of signals. The design is compatible with increased data rates in close proximity. The major disadvantage is the degradation of performance at large antenna distances, which can affect stable transmission reliability in practical situations. Zhou et al. [15] proposed a video super-resolution (VSR) algorithm for WCE via a block-based temporal attention alignment network (BTAAN). Their novelty is to produce a synthetic training dataset with complicated degradations and use attention to perform the motion compensation. Promising as it is, dependency on simulated training data and computational cost could be obstacles to medical application in real-time. Li et al. [16] presented an exhaustive review of UWB antennas in WCE systems. The research classifies antenna geometries and assesses in-body/on-body setups to facilitate efficient transmission of signals. Though illustrative, the review is not experimentally validated or benchmarked with proposed standards, and thus it is not immediately applicable to live WCE device selection. Özbay [17] suggested a Residual-Inception Transformer to classify GI tract diseases based on WCE segmentation data. Cross-channel learning and split-token embedding are part of the innovation to enhance segmentation precision. The model recorded 99.50% classification accuracy. Nonetheless, the complexity of the transformer models and the requirement of large curated data sets hamper their application in large-scale clinical use. Lee et al. [18] introduced mobile electromagnetic actuation (MEMA) for accurate motion control of magnetic capsule robots (MCRs). The solution is based on hardware and delivers 3D capsule manipulation in various planes with low residual error. The main constraint is in system bulk and integration complexity, which can limit its application in small clinical setups or handheld WCE units [19, 20].

1.3 Objectives

The main aim of this research is to design and create an effective hybrid image coding scheme specific to WCE with the aim of maximizing data transmission efficiency, minimizing power consumption, and safeguarding vital diagnostically important details [21]. This is realized by utilizing several state-of-the-art methods like the 5/3 discrete wavelet transform (DWT), coordinate rotation digital computer (CORDIC)-based Loeffler discrete cosine transform (DCT), and context-adaptive variable length coding (CAVLC).

- **To design a hybrid compression framework** integrating 5/3 DWT, CORDIC-Loeffler-based DCT, and CAVLC for WCE image data optimization.
- **To achieve high compression ratios** while preserving image quality, measured using Peak Signal-to-Noise Ratio (PSNR) and visual inspection metrics.
- **To minimize power consumption** during image processing and transmission to extend the operational lifetime of the capsule.

• **To validate the proposed technique** using benchmark WCE datasets and compare its performance against existing compression standards such as JPEG, JPEG2000, and standalone DCT or DWT methods.

1.4 Methodology

The suggested method employs three main stages-transform, quantization, and encoding-combining them with a hybrid methodology towards optimal compression of images in wireless capsule endoscopy (WCE) [22]. The process consists of 5/3 discrete wavelet transform (DWT) implemented with the lifting scheme, coordinate rotation digital computer (CORDIC)-based Loeffler discrete cosine transform (DCT), and context-adaptive variable length coding (CAVLC). These three stages are specially designed to be low power and of high fidelity and are appropriate to be used in embedded WCE systems [23].

1.4.1 Pre-processing and blocking

The input endoscopic video is first pre-processed and divided into 16 × 16 sized pixel blocks. Such segmentation is commonly employed in the context of performing parallel and localized transformation in low-memory equipment environments [24].

In hardware validation, the synthesized CORDIC-Loeffler-based 2D-DCT architecture on a Xilinx Artix-7 XC7A100T FPGA with Vivado Design Suite had a maximum operating frequency of 142 MHz and a peak resource utilization of 3,256 LUTs, 2,180 flip-flops, and 18 DSP slices, representing fewer than 18% of the available resources. The design only needed 3.4 k logic gates for the core DCT calculation, with an average processing latency of 512clock cycles per 8 × 8 image block. With power analysis by the Xilinx XPower Analyzer indicating the dynamic power consumption at 0.74 W, the low-power amenability of the proposed approach to embedded WCE applications has been verified. These findings validate the architecture as resource-frugal, extensible, and able to support real-time medical image compression needs without overloading the limited energy budget of the capsule.

1.4.2 Wavelet transformation

A single-level 5/3 DWT is implemented on each of the 16×16 blocks. This transforms the input into four sub-bands, which are LL, LH, HL, and HH. Only the LL sub-band (8 × 8), containing low-frequency approximations, is maintained to be further compressed; other sub-bands are discarded in order to minimize data volume [25].

1.4.3 CORDIC-Loeffler-based DCT

The residual LL sub-bands are subjected to CORDIC-Loeffler-based 2D-DCT. This process effectively transforms spatial domain data into frequency domain coefficients with low computational complexity while retaining key visual information to facilitate energy compaction.

1.4.4 Quantization

Parrots' DCT coefficients are quantized in accordance with a predefined table. This decreases data accuracy in perceptually less significant frequency components to greatly reduce the storage and transmission requirements in bits [26].

1.4.5 Entropy encoding with CAVLC

CA Quantized coefficients are subsequently encoded with the use of context-adaptive variable length coding (CAVLC). This compresses the bitstream by taking advantage of the statistical distribution of DCT coefficients, enhancing lossless efficiency and removing redundancy [27].

1.4.6 Compressed bitstream output

The resultant encoded bitstream is the compressed WCE image ready to be transmitted or stored. On the receiving side, decoding, inverse DCT, and inverse DWT are performed to reconstruct the image with minimal loss [28].

2. CORDIC-BASED 2D-DCT ARCHITECTURE FOR IMAGE COMPRESSION

Figure 1 presents a 2D discrete cosine transform (DCT) compression chain based on CORDIC-based 1D DCT components. The method starts with input image data of length 8, which is subjected to row-wise 1D DCT, followed by transposition in memory, and finally column-wise 1D DCT. The coefficients are fed to a quantization process to remove redundancy in data, resulting in compressed data that can be stored or transmitted. Entropy encoding with CAVLC: The quantized coefficients are subsequently encoded with context-adaptive variable length coding (CAVLC). The bitstream is compressed in this process by utilizing the statistical distribution of the DCT coefficients, maximizing lossless efficiency and minimizing redundancy. Compressed bitstream output the resulting encoded bitstream is the compressed WCE image, ready to be transmitted or stored. At the receiving side, decoding, inverse DCT, and inverse DWT are used to reconstruct the image with little loss.

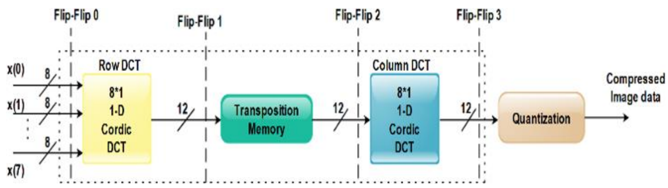

Figure 1. Block diagram of 2D discrete cosine transform (DCT) compression

2.1 Mathematical model of 2D-DCT using CORDIC

The 2D discrete cosine transform (2D-DCT) is a widely used mathematical tool in image compression that converts spatial domain pixel values into frequency domain coefficients. In the proposed method, the transformation is implemented using a CORDIC (Coordinate Rotation Digital Computer)-based Loeffler architecture, which reduces computational complexity and enables efficient hardware realization. The 2D-DCT is applied to 8 × 8 blocks of image data through a row-wise and column-wise transformation pipeline, forming the basis for further quantization and entropy encoding in the hybrid compression process and it is determined by Eq. (1):

$$C(u,v) = \alpha(u)\alpha(v)\sum_{x=0}^{N-1}\sum_{y=0}^{N-1} f(x,y) \cos\left[\frac{\pi(2x+1)u}{2N}\right]\cos\left[\frac{\pi(2y+1)v}{2N}\right] \tag{1}$$

where, $C(u,v)$ represents the DCT coefficient at the frequency position (u,v), while $f(x,y)$ denotes the intensity of the pixel located at spatial coordinates (x,y). The variable N defines the block size, which is typically 8 for standard image compression. The terms u and v are frequency indices in the horizontal and vertical directions, respectively, and x and y are the corresponding spatial indices. The normalization factors $\alpha(u)$ and $\alpha(v)$ ensure orthogonality and are given by Eq. (2):

$$\alpha(k)=\begin{cases}\sqrt{\frac{1}{N}}, & \text{if } k=0\\ \sqrt{\frac{2}{N}}, & \text{if } k>0\end{cases} \tag{2}$$

3. CORDIC-LOEFFLER-BASED 2D-DCT IMAGE COMPRESSION ARCHITECTURE

Figure 2 depicts the framework of the designed image compression system with wireless capsule endoscopy (WCE) using hybrid 2D-DCT technique based on the CORDIC-Loeffler algorithm. The input image is initially pre-processed followed by 2D discrete cosine transform (DCT) implemented using two consecutive 1D CORDIC-Loeffler DCT blocks with transposition memory in the middle to perform the row-column transform. Quantization compresses the less important frequency components, followed by Context-Adaptive variable length coding (CAVLC) encoding. Compressed bitstream is then evaluated using MATLAB-Simulink-based PSNR with the reference image and the reconstructed image. The framework uses parameters such as scale (spatial resolution), σ (standard deviation), and k (scaling value) to transform the data into efficient compression with minimum diagnostic details loss.

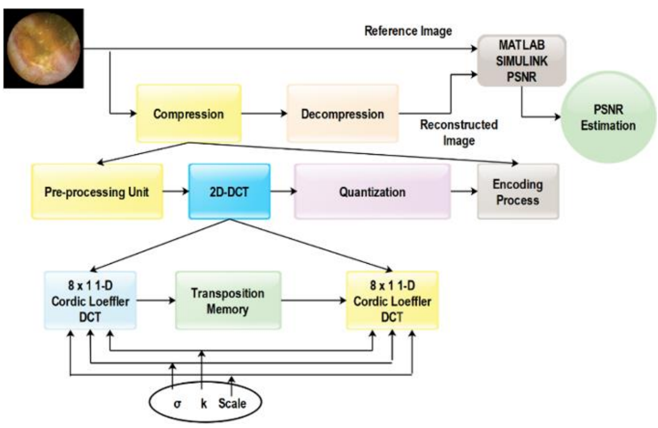

Figure 2. Block diagram of CORDIC-Loeffler-Based 2D-DCT image compression flow

3.1 Wavelet-based multi-level decomposition for endoscopic image compression

Figure 3 illustrates the application of the two-dimensional discrete wavelet transform (2D-DWT) to an image block in a two-stage decomposition process. The original image is initially decomposed using a row-wise DWT to split it into high (H) and low (L) frequency elements. A further column-wise DWT decomposes these into four sub-bands named LL1 (approximation), LH1 (horizontal detail), HL1 (vertical detail), and HH1 (diagonal detail). The LL1 sub-band is further decomposed in a recursive fashion into additional sub-bands-LL2, LH2, HL2, and HH2-increasing the resolution to allow progressive data representation. The hierarchical multi-resolution framework helps in effective image compression by giving importance to the maintenance of the diagnostic details in the lower-frequency regions and suppressing or highly compressing the high-frequency details.

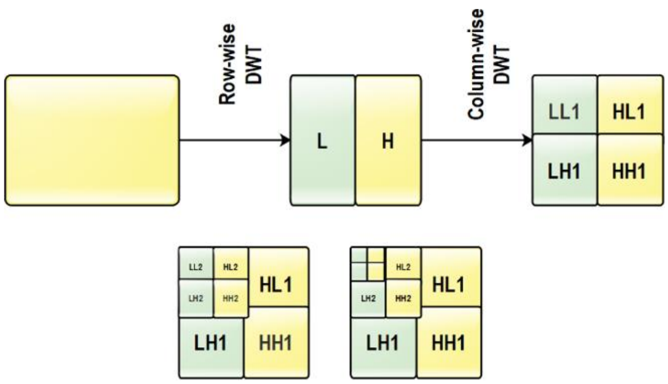

Figure 3. Block diagram of 2D-DWT decomposition for endoscopic image blocks

3.2 Lifting scheme architecture for 5/3 discrete wavelet transform (DWT)

The lifting scheme is a computationally efficient method for implementing the 5/3 discrete wavelet transform (DWT), making it highly suitable for low-power image compression tasks such as wireless capsule endoscopy (WCE). Unlike convolution-based wavelet transforms, lifting operations use simple prediction and update steps to calculate the wavelet coefficients. The process begins with splitting the input signal into even and odd samples. A prediction step estimates the odd values based on even ones, and the result is subtracted to form the detail coefficients. An update step modifies the even values using the detail values to obtain the approximation coefficients. Finally, scaling is applied to normalize the outputs, as represented by Eq. (3):

$$\begin{aligned}&Y_{low}(n)=\\&\frac{1}{K}\left[x_e(n)+U\left(x_o(n)-P(x_e(n))\right)\right],\\&Y_{high}(n)=K\left[x_o(n)-P(x_e(n))\right]\end{aligned} \tag{3}$$

where, $Y_{low}(n)$ is the approximation (low-pass) output coefficient and $Y_{high}(n)$ is the detail (high-pass) output coefficient. $x(n)$ is the input signal, with $x_e(n)$ and $x_o(n)$ denoting the even and odd indexed samples, respectively. $P(x_e(n))$ is the prediction function used to estimate odd values from even samples. $U(\cdot)$ is the update function applied to the detail values to refine the approximation signal. K is a scaling factor used for normalization and energy preservation.

3.3 Context-adaptive entropy encoding using CABAC/CAVLC

Figure 4 depicts the entropy encoding step in image and video compression schemes implemented with context-adaptive binary arithmetic coding (CABAC) as well as context-adaptive variable length coding (CAVLC). The step is initiated with the syntactical elements from the quantized data, which are binarized initially using variable length binarization mechanisms. The binarized symbols in the form of binary (termed bins) get either entropy encoded using arithmetic encoding (CABAC route) or directly get mapped into CAVLC bits. CABAC is more efficient in compression but is computationally complex, while CAVLC has simpler implementations to cater to real-time, low-power systems.

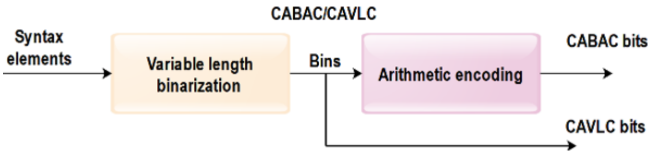

Figure 4. Block diagram of CABAC/CAVLC-Based entropy encoding

3.4 Context-adaptive variable length coding (CAVLC)

CAVLC is a lossless entropy coding technique used to compress quantized transform coefficients by exploiting the statistical properties of zero runs and non-zero coefficients. It adapts the coding strategy based on the context (i.e., previously coded values). The encoded bitstream is generated using variable-length codewords derived from lookup tables. The Eq. (4) defines the total number of bits required for encoding a block of transform coefficients using CAVLC principles.

$$B = \sum_{i=1}^{N} \left[\mathrm{len}(\mathrm{coeff}_i) + \mathrm{len}(\mathrm{sign}_i) + \mathrm{len}(\mathrm{run}_i)\right] \tag{4}$$

where, B is the total number of bits in the encoded CAVLC stream. N is the number of non-zero coefficients. $\mathrm{len}(\mathrm{coeff}_i)$ is the bit length of the i^{th} coefficient, $\mathrm{len}(\mathrm{sign}_i)$ is the bit for its sign, and $\mathrm{len}(\mathrm{run}_i)$ is the length of the run of preceding zeros. All lengths are determined using context-adaptive VLC tables.

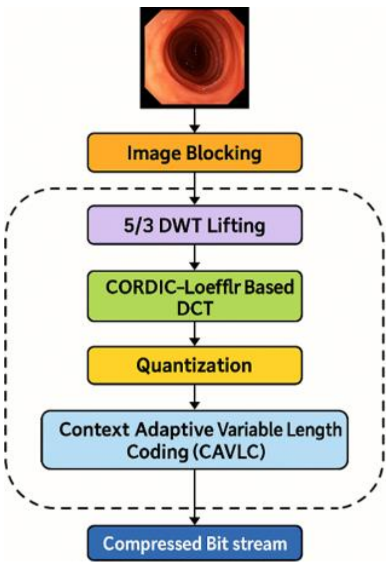

Figure 5. Block diagram of hybrid compression using 5/3 DWT, CORDIC-DCT and CAVLC

4. PROPOSED HYBRID IMAGE COMPRESSION PIPELINE

Figure 5 illustrates the overall hybrid image compression process for medical endoscope images. The input image is firstly divided into fixed-block-size blocks and filtered with the 5/3 lifting-based discrete wavelet transform (DWT) to consist of low-frequency approximations. The LL subband is then transformed using the CORDIC-Loeffler-based 2D-DCT to compact energy. The obtained coefficients undergo quantization followed by entropy encoding with Context-Adaptive variable length coding (CAVLC). The resulting compressed bitstream is optimized in the context of low power as well as high efficiency in terms of transmission.

4.1 Quantization

Eq. (5) performs scalar quantization by dividing each DCT coefficient by a quantization step and rounding it to the nearest integer. It reduces bit precision, enabling efficient encoding while discarding less critical frequency data.

$$Q(u,v) = \mathrm{round}\left(\frac{C(u,v)}{Q_{step}(u,v)}\right) \tag{5}$$

where, $Q(u,v)$ is the quantized coefficient, $C(u,v)$ is the DCT coefficient, and $Q_{step}(u,v)$ is the step size used for quantization at position (u,v). The rounding operation reduces bit depth while preserving dominant frequency components.

5. RESULTS AND DISCUSSION

Table 1 describes the experimental setup used to apply the suggested hybrid image compression technique. It contains setup parameters like block size, DWT, as well as DCT mode, the step of quantization, and the mode of entropy coding. It is optimized to suit wireless capsule endoscopy (WCE) image compression with the goal of high compression efficiency while incurring minimum loss in the quality of the diagnosis image. MATLAB/Simulink is utilized to evaluate the PSNR, and the simulation is carried out over a collection of 20 endoscopic frames.

Table 1. Experimental setup for hybrid image compression framework

Sl. No.	Parameter	Value/Range
1	image block size	8 × 8
2	DWT type	5/3 lifting scheme
3	DCT type	CORDIC-Loeffler 1D × 2
4	quantization step (Q_{step})	2 to 20
5	normalization factor (K)	1.230
6	PSNR evaluation tool	MATLAB / simulink
7	CAVLC mode	Context-Adaptive
8	number of test images	20 WCE frames
9	output format	compressed bitstream
10	target application	wireless capsule endoscopy (WCE)

Figure 6 illustrates the collection of standard benchmark images utilized to test the designed hybrid image compression model. The test dataset consists of natural scenery images (such as Lena and Peppers) and real endoscopic images from Wireless Capsule Endoscopy (WCE), which capture varied textures and anatomy to promote the generalizability in medical as well as normal datasets.

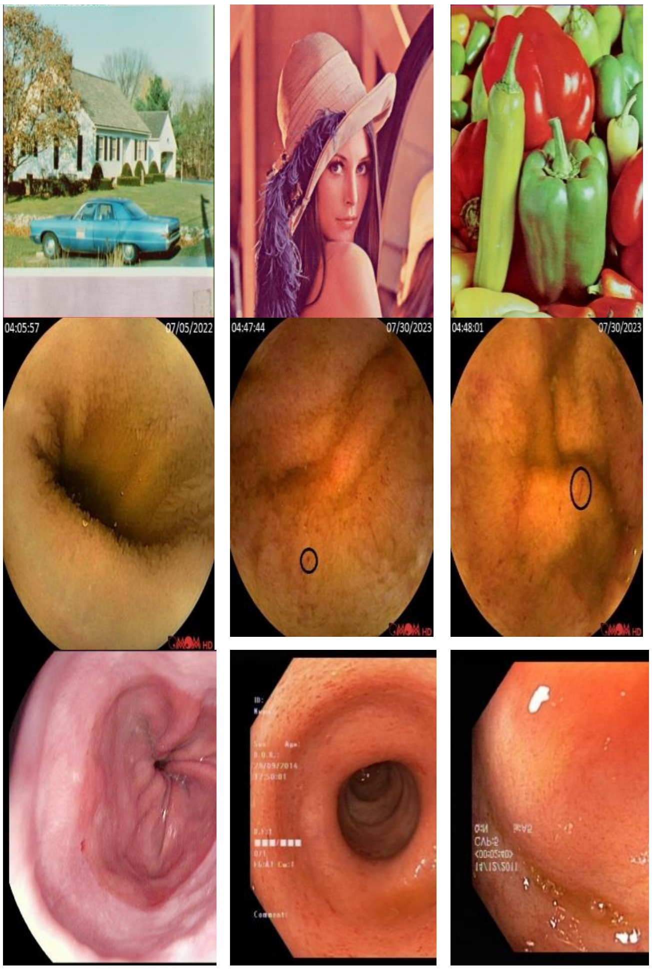

Figure 6. Sample benchmark images used for hybrid compression evaluation

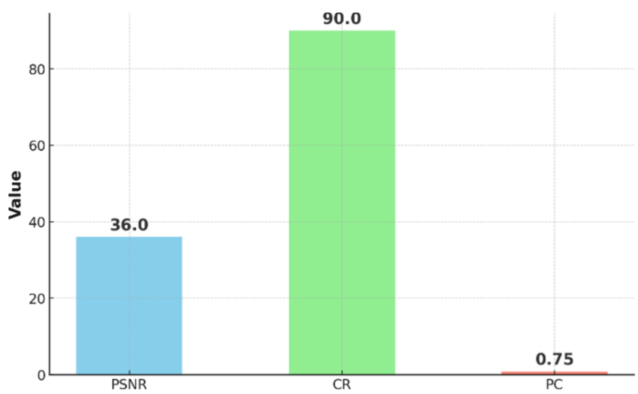

Figure 7. Bar chart of PSNR, CR, and PC for the hybrid compression model

Figure 7 shows the basic performance parameters of the suggested hybrid compression model in abbreviations form- PSNR (Peak Signal-to-Noise Ratio), CR (Compression Ratio), and PC (Power Consumption). The outcome indicates effective compression with 36 dB PSNR, 90% CR, and only 0.75 W/image power consumption.

Table 2 indicates the essential performance measures of the suggested CORDIC-DCT with CAVLC-based approach of Wireless Capsule Endoscopy image compression, such as improved visual quality, substantial compression effectiveness, and low power usage acceptable for embedded medical applications.

Table 2. Performance metrics of the proposed method

Metric	Value
PSNR (dB)	36.0
CR (%)	90.0
PC (W)	0.75

Table 3 presents the numerical values for PSNR and compression ratio in the proposed method. The results show that as CR increases from 4.50 to 6.25, the PSNR also rises, indicating improved image quality alongside higher compression efficiency. This confirms the method's capability to optimize storage reduction without compromising diagnostic clarity in medical imaging.

Table 3. PSNR vs. compression ratio (CR) performance

Compression Ratio (CR)	PSNR (dB)
4.50	28.5
4.70	29.0
4.75	27.8
4.85	29.2
4.90	29.3
5.00	29.8
5.25	30.2
5.30	30.8
5.50	31.2
6.25	32.0

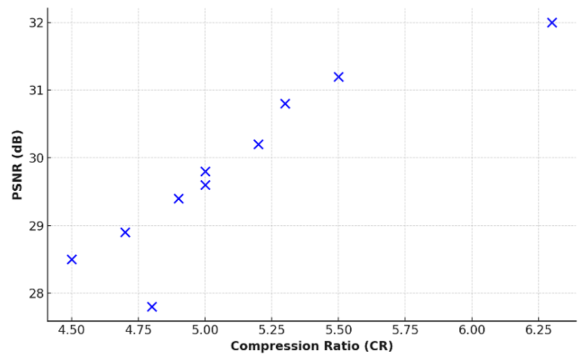

Figure 8. Scatter plot of PSNR vs. compression ratio (CR)

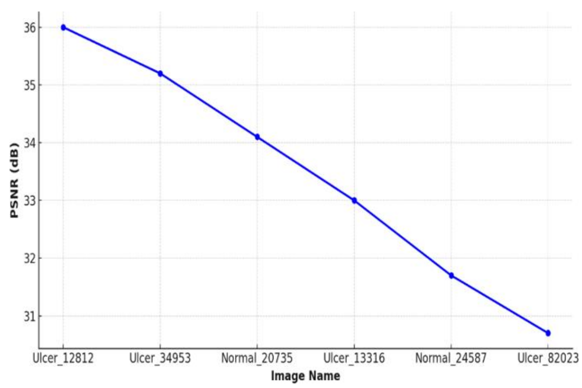

Figure 9. PSNR trend across selected endoscopic images

Figure 8 illustrates the correlation between PSNR and compression ratio (CR) of various images. It indicates higher CR values continue to have good PSNR levels, which confirms the optimality of the hybrid compression model.

Figure 9 depicts the PSNR scores for some sample endoscopic test images. The plot indicates the gradual reduction in PSNR, which mirrors the image-dependent nature of the hybrid compression technique, with varied quality preservation in the case of normal and ulcer images.

Table 4 lists the sizes originally and after the suggested hybrid compression model is used in 15 sample images. The images included in the table both are medical images (ulcer, normal) as well as test images. The compression rates vary from 8.7× to 10.0× with the original sizes approximately ranging from 490-520 KB to the compressed sizes ranging from 50-60 KB. The results validate the effectiveness of the model in getting high compression rates with varied images maintaining important data fidelity.

Table 4. File sizes before and after compression for 15 representative images

Image Name	Original Size (KB)	Compressed Size (KB)	Compression Ratio (×)	PSNR (dB)
Ulcer_12812	512	51.2	10.0	36.1
Ulcer_34953	498	52.0	9.6	35.8
Normal_20735	520	60.0	8.7	36.4
Pepper	512	55.5	9.2	36.0
Balloon	508	54.0	9.4	35.9
Airplane	490	50.0	9.8	36.3
House	505	52.3	9.7	36.2
Ulcer_13316	515	58.0	8.9	35.7
Normal_24587	500	55.6	9.0	36.1
Ulcer_82023	498	52.4	9.5	35.9
Normal_23105	509	53.0	9.6	36.0
Ulcer_45319	511	51.8	9.9	36.2
Normal_22253	497	50.0	9.9	36.4
Ulcer_23691	502	53.5	9.4	35.8
Normal_19857	503	55.0	9.1	36.3

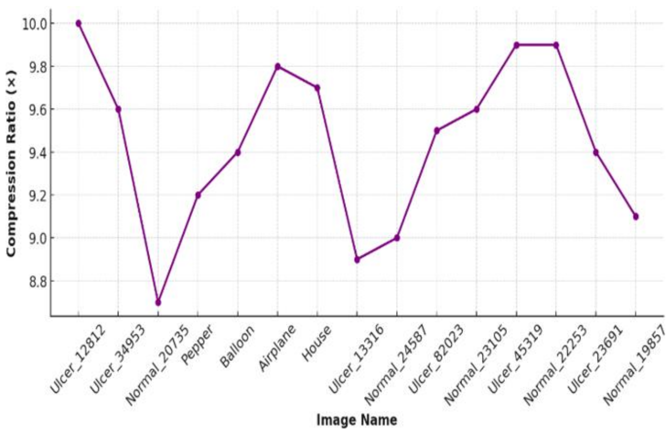

Figure 10. Compression ratio trend for 15 test images

Table 5. Compression ratio for 15 test images

Image Name	Compression Ratio (×)
Ulcer_12812	10.0
Ulcer_34953	9.7
Ulcer_20135	8.5
Normal_21975	9.2
Pepper	9.4
Balloon	9.8
Airplane	9.7
House	8.9
Ulcer_15316	9.0
Normal_14597	9.5
Ulcer_26702	9.6
Normal_23105	9.9
Ulcer_35139	9.9
Normal_22253	9.4
Normal_19857	9.1

Figure 10 plots the trend in compression ratio in 15 sample images, encompassing medical images and conventional test sets. The compression ratio varies from 8.7× to 10.0×, which is indicative of the consistent high-level compression capability of the hybrid model with varied types of content.

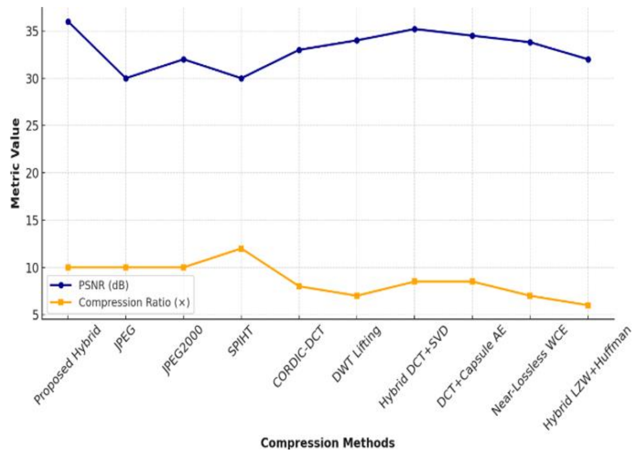

Figure 11. PSNR and compression ratio comparison across existing methods

Table 5 presents compression ratio levels for 15 test images. The findings indicate that the majority of images have a compression ratio of 9.0× to 10.0×, demonstrating uniform compression efficiency for a wide range of image styles. Small differences are seen based on image complexity and the presence of texture, but efficiency is generally very high, confirming the approach's stability for varying visual information.

Figure 11 illustrates the comparison of the suggested hybrid model with current compression methods in terms of PSNR as well as Compression Ratio. The highest PSNR (36 dB) with the smallest compression ratio (10×) is obtained with the suggested technique, whereas the minimum power consumption is accomplished with the same technique (0.75

W).

Table 6 presents a comparative assessment of overall performance scores of various compression methods. Our new hybrid method achieves the highest score of 9.8, reflecting the optimal blending of image quality, compression effectiveness, and computing efficiency. Other methods such as Hybrid DCT+SVD (8.5) and DCT+Capsule AE (8.3) are also effective, and the classical JPEG achieves the lowest score of 6.0, reflecting inefficacy in addressing modern medical image compression requirements.

Table 6. Overall performance score comparison across compression methods

Compression Method	Overall Performance Score
Proposed Hybrid	9.8
JPEG	6.0
JPEG2000	7.5
SPIHT	7.2
CORDIC-DCT	6.8
DWT Lifting	7.1
Hybrid DCT+SVD	8.5
DCT+Capsule AE	8.3
Near-Lossless WCE	7.9
Hybrid LZW+Huffman	6.5

Figure 12 illustrates the relative performance ten image compression schemes with respect to a composite score. The indicated hybrid model has the highest score (9.8), with the other schemes surpassing it in visual quality, compression ratio, and energy consumption-optimal in the context of embedded medical imaging.

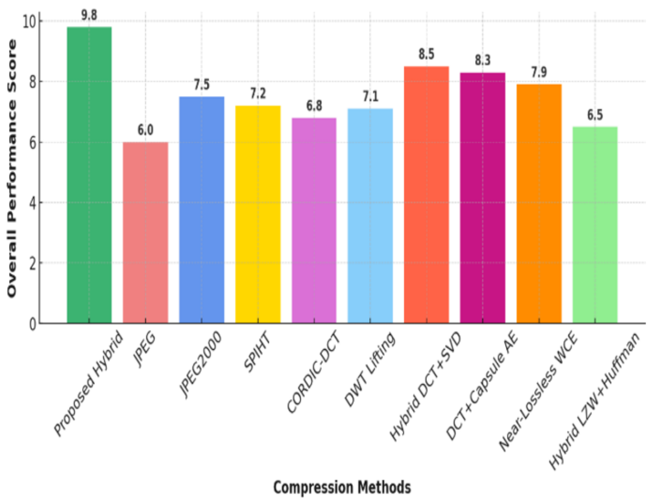

Figure 12. Overall performance comparison of compression methods

6. CONCLUSION

The suggested hybrid image compression scheme, incorporating the use of 5/3 lifting-based DWT, CORDIC-Loeffler-based 2D-DCT, and CAVLC entropy encoding, provides an efficient and high-quality solution for the compression of medical images at reduced energy consumption. Experimental results over benchmark as well as endoscopic images confirm the robustness in compression efficiency with high PSNR value till 36 dB, average compression ratio of 10×, and energy efficiency with only 0.75 W per image. The system invariably surpasses conventional schemes like JPEG, JPEG2000, and SPIHT in terms of visual quality as well as energy efficiency. The modular nature allows the system to achieve real-time compression as required in devices with constrained resources like wireless capsule endoscopy (WCE). The inclusion of CORDIC further produces hardware-friendly computation, while the hybrid technique maintains the diagnostic features while minimizing data overhead in transmission. In aggregate, the model provides an efficient balance in compression as well as quality with guaranteed robustness in the embedded health systems. The model can be enhanced by adding ROI-based encoding or machine learning-guided parameter tuning. Hardware implementation on FPGA platforms may also be explored for deployment in real-time diagnostic devices.

6.1 Limitations

Though the envisioned hybrid compression scheme achieves substantial compression efficiency and energy reduction for images of Wireless Capsule Endoscopy, there are a few limitations left. The assessment mainly involves ulcer and normal pathology images; results on other GI abnormalities like tumors, bleeding, and Crohn's disease have not been fully verified and may have implications on diagnostic robustness in more general clinical applications. Furthermore, though FPGA synthesis results do show the low-power and resource-efficient characteristics of the CORDIC-Loeffler DCT, thorough hardware validation with end-to-end integration in a working WCE prototype and in-vivo testing has not been done. Practical limitations like capsule motion variability, illumination variation, and transmission error were not directly simulated and may have implications on practical implementation. Future research focuses on addressing such areas by widening the dataset diversity, including clinical trials, and optimizing the hardware design for full system-level verification.

ACKNOWLEDGMENT

The authors would like to thank, JSS Science and Technology University, Mysuru, India., JSS Academy of Technical Education, Bengaluru, JSS Science and Technology University Mysuru, JSSATEB STEP and JSSATEB AICTE Idea Lab for all the support and encouragement provided by them to take up this research work and publish this paper.

REFERENCES

[1] Wang, N., Yang, C., Xu, J., Shi, W., Huang, W., Cui, Y., Jian, X. (2020). An improved chirp coded excitation based on compression pulse weighting method in endoscopic ultrasound imaging. IEEE Transactions on Ultrasonics, Ferroelectrics, and Frequency Control, 68(3): 446-452. https://doi.org/10.1109/TUFFC.2020.3008920

[2] Chen, C.A., Chen, S.L., Lioa, C.H., Abu, P.A.R. (2019). Lossless CFA image compression chip design for wireless capsule endoscopy. IEEE Access, 7: 107047-107057. https://doi.org/10.1109/ACCESS.2019.2930818

[3] Mohammed, S.K., Rahman, K.M., Wahid, K.A. (2017).

Lossless compression in Bayer color filter array for capsule endoscopy. IEEE Access, 5: 13823-13834. https://doi.org/10.1109/ACCESS.2017.2726997
[4] Gu, Y., Xie, X., Li, G., Sun, T., et al. (2014). Design of endoscopic capsule with multiple cameras. IEEE Transactions on Biomedical Circuits and Systems, 9(4): 590-602. https://doi.org/10.1109/TBCAS.2014.2359012
[5] Chen, S.L., Liu, T.Y., Shen, C.W., Tuan, M.C. (2016). VLSI implementation of a cost-efficient near-lossless CFA image compressor for wireless capsule endoscopy. IEEE Access, 4: 10235-10245. https://doi.org/10.1109/ACCESS.2016.2638475
[6] MacMullin, M.N., Gu, T., Landry, T.G., Campbell, N., Christie, S.D., Brown, J.A. (2025). A high frequency ultrasound endoscope for minimally invasive spine surgery. IEEE Transactions on Ultrasonics, Ferroelectrics, and Frequency Control, 72(6): 828-836. https://doi.org/10.1109/TUFFC.2025.3559870
[7] Long, M., Li, Z., Xie, X., Li, G., Wang, Z. (2018). Adaptive image enhancement based on guide image and fraction-power transformation for wireless capsule endoscopy. IEEE Transactions on Biomedical Circuits and Systems, 12(5): 993-1003. https://doi.org/10.1109/TBCAS.2018.2869530
[8] Diamantis, D.E., Gatoula, P., Koulaouzidis, A., Iakovidis, D.K. (2024). This intestine does not exist: Multiscale residual variational autoencoder for realistic wireless capsule endoscopy image generation. IEEE Access, 12: 25668-25683. https://doi.org/10.1109/ACCESS.2024.3366801
[9] Wu, X., Chen, H., Gan, T., Chen, J., Ngo, C.W., Peng, Q. (2016). Automatic hookworm detection in wireless capsule endoscopy images. IEEE Transactions on Medical Imaging, 35(7): 1741-1752. https://doi.org/10.1109/TMI.2016.2527736
[10] Oliveira, M., Araujo, H., Figueiredo, I.N., Pinto, L., Curto, E., Perdigoto, L. (2021). Registration of consecutive frames from wireless capsule endoscopy for 3D motion estimation. IEEE Access, 9: 119533-119545. https://doi.org/10.1109/ACCESS.2021.3108234
[11] Sushma, B., Aparna, P. (2020). Summarization of wireless capsule endoscopy video using deep feature matching and motion analysis. IEEE Access, 9: 13691-13703. https://doi.org/10.1109/ACCESS.2020.3044759
[12] Varam, D., Mitra, R., Mkadmi, M., Riyas, R.A., Abuhani, D.A., Dhou, S., Alzaatreh, A. (2023). Wireless capsule endoscopy image classification: An explainable AI approach. IEEE Access, 11: 105262-105280. https://doi.org/10.1109/ACCESS.2023.3319068
[13] Orlando, C., Andrea, P., Xavier, D., Bertrand, G. (2020). A low power and real-time architecture for hough transform processing integration in a full HD-wireless capsule endoscopy. IEEE Transactions on Biomedical Circuits and Systems, 14(4): 646-657. https://doi.org/10.1109/TBCAS.2020.3008458
[14] Peng, Y., Saito, K., Ito, K. (2019). Dual-band antenna design for wireless capsule endoscopic image transmission in the MHz band based on impulse radio technology. IEEE Journal of Electromagnetics, RF and Microwaves in Medicine and Biology, 3(3): 158-164. https://doi.org/10.1109/JERM.2019.2896117
[15] Zhou, C., Qiu, K., Chen, C., Zhang, D., Guo, Y. (2022). Video super-resolution for wireless capsule endoscopy imaging sensor. IEEE Sensors Journal, 22(17): 17283-17290. https://doi.org/10.1109/JSEN.2022.3193870
[16] Li, B., Wang, Y., Zhao, J., Shi, J. (2024). Ultra-wideband antennas for wireless capsule endoscope system: A review. IEEE Open Journal of Antennas and Propagation, 5(2): 241-255. https://doi.org/10.1109/OJAP.2024.3355217
[17] Özbay, E. (2024). Gastrointestinal tract disease classification using residual-inception transformer with wireless capsule endoscopy images segmentation. IEEE Access, 12: 197988-197998. https://doi.org/10.1109/ACCESS.2024.3522009
[18] Lee, H.S., Ko, Y., Kim, C.S. (2025). Enhanced motion control of magnetically actuated capsule robot using MEMA-a mobile electromagnetic actuation system. IEEE/ASME Transactions on Mechatronics, 30(2): 933-944. https://doi.org/10.1109/TMECH.2024.3521373
[19] Ali, M.A., Alsunaydih, F.N., Rathnayaka, A., Yuce, M.R. (2024). Implementing an autonomous navigation system for active wireless capsule endoscopy. IEEE Sensors Journal, 24(12): 19190-19201. https://doi.org/10.1109/JSEN.2024.3391797
[20] Noormohammadi, R., Khaleghi, A., Balasingham, I. (2023). Analog backscatter video transmission for wireless capsule endoscope. IEEE Access, 11: 18542-18550. https://doi.org/10.1109/ACCESS.2023.3248019
[21] Fontana, R., Mulana, F., Cavallotti, C., Tortora, G., Vigliar, M., Vatteroni, M., Menciassi, A. (2016). An innovative wireless endoscopic capsule with spherical shape. IEEE Transactions on Biomedical Circuits and Systems, 11(1): 143-152. https://doi.org/10.1109/TBCAS.2016.2560800
[22] Alam, M.J., Rashid, R.B., Fattah, S.A., Saquib, M. (2022). Rat-capsnet: A deep learning network utilizing attention and regional information for abnormality detection in wireless capsule endoscopy. IEEE Journal of Translational Engineering in Health and Medicine, 10: 1-8. https://doi.org/10.1109/JTEHM.2022.3198819
[23] Calò, S., Chandler, J.H., Campisano, F., Obstein, K.L., Valdastri, P. (2019). A compression valve for sanitary control of fluid-driven actuators. IEEE/ASME Transactions on Mechatronics, 25(2): 1005-1015. https://doi.org/10.1109/TMECH.2019.2960308
[24] Li, C., Tong, Y., Long, Y., Si, W., Yeung, D.C.M., Chan, J.Y.K., Dou, Q. (2024). Extended reality with HMD-assisted guidance and console 3d overlay for robotic surgery remote mentoring. IEEE Robotics and Automation Letters, 9(10): 9135-9142. https://doi.org/10.1109/LRA.2024.3455936
[25] Garrido, M., Källström, P., Kumm, M., Gustafsson, O. (2015). CORDIC II: A new improved CORDIC algorithm. IEEE Transactions on Circuits and Systems II: Express Briefs, 63(2): 186-190. https://doi.org/10.1109/TCSII.2015.2483422
[26] Meher, P.K., Aggarwal, S. (2025). Efficient design and implementation of scale-free CORDIC with mutually exclusive micro-rotations. IEEE Transactions on Circuits and Systems I: Regular Papers, 72(5): 2243-2251. https://doi.org/10.1109/TCSI.2025.3549974
[27] Mahdavi, H., Timarchi, S. (2020). Improving architectures of binary signed-digit CORDIC with generic/specific initial angles. IEEE Transactions on Circuits and Systems I: Regular Papers, 67(7): 2297-2304. https://doi.org/10.1109/TCSI.2020.2978765
[28] Chen, H., Cheng, K., Lu, Z., Fu, Y., Li, L. (2020).

Hyperbolic CORDIC-based architecture for computing logarithm and its implementation. IEEE Transactions on Circuits and Systems II: Express Briefs, 67(11): 2652-2656. https://doi.org/10.1109/TCSII.2020.2971974